VDMA
Fluid Power Association

22nd ISC

International Sealing Conference

Stuttgart, Germany
October 01 - 02, 2024

Sealing Technology –
Challenges accepted!

IMA UNI STUTTGART

ISBN 978-3-8163-0768-6

Fachverband Fluidtechnik im VDMA e. V. Lyoner Str. 18
50628 Frankfurt am Main
Germany

Phone +49 69 6603-1513
E-Mail maximilian.baxmann@vdma.org
Internet www.vdma.org/fluid

A smart seal energizer from shape-memory-alloy

Anne Marie Lehmann, Anja Dobrinsky, Martin Franz

Harsh operating conditions can significantly shorten a seal's lifetime, potentially harming people and the environment. One effective solution to this challenge is the adoption of actuatable seals that can adapt to varying operating conditions. Shape-memory-alloys (SMA) serve as ideal actuators for polymer seals, thanks to their high operating displacement, relatively low tension load and flexible design capabilities. This work presents a proof of concept for a polytetrafluoroethylene (PTFE) rod seal energized by a SMA wire. The wire is coiled around the seal's outer circumference and activated through induction. Upon activation, the wire contracts, thereby increasing the seal's radial load. The adjustable radial load allows the sealing function and friction properties to be precisely tailored to the specific operating conditions in application.

1 Introduction

Global changes, such as Industry 4.0 [1], climate change and increasing individualization, demand flexibility and adaptation. In modern technical systems, harsh operating conditions already challenge the longevity of seals. A crucial factor for a seal's lifespan in dynamic application is the optimal distribution of contact pressure. Typically, sealing solutions employ energizers like metal springs or elastomer O-Rings to ensure and maintain adequate contact pressure. There are primarily two conventional approaches for energizers in dynamic sealing systems: the inherent elasticity of sealing materials and the additional use of steel springs.

Some sealing solutions can adapt passively to varying operating conditions through mechanisms such as thermal expansion [2] and centripetal forces that cause displacement and deformation [3]. Nevertheless, the lifetime of sealing systems is finite always subject to improvement. Actively adapting a sealing system using smart materials represents a promising third approach to optimally adjust contact pressure and extend a seal's lifetime.

SMAs are well-known smart materials and have exceptional displacement and restoring properties [4]. This paper explores how a SMA can be utilized to regulate the contact pressure of a sealing profile, potentially enhancing the overall performance and durability of sealing systems.

2 Theoretical background

2.1 Dynamic Seals

Dynamic seals are essential components in various mechanical systems, ensuring the containment of fluids or gases while permitting relative motion between parts.

Unlike static seals, which remain stationary, dynamic seals must accommodate movement without compromising integrity.

As depicted in Figure 1, a basic dynamic seal comprises a movable seal body (SB) and a surface in motion (MS) that moves relative to the seal body. The primary sealing interface (P) is formed between the mating seal faces. The gap at this interface, known as the "seal gap" or "film thickness," is extremely narrow, typically measured in micrometers (μm).

The secondary sealing interface (S) prevents leakage between the seal body and the housing (H). This is achieved by applying a closing force (F), which reduces clearance at both the primary and secondary sealing interfaces. Additionally, a retention device (R) prevents the seal body from slipping due to friction with the moving surface. In more complex sealing systems, a second sealing body often forms an additional secondary sealing interface (S) [2].

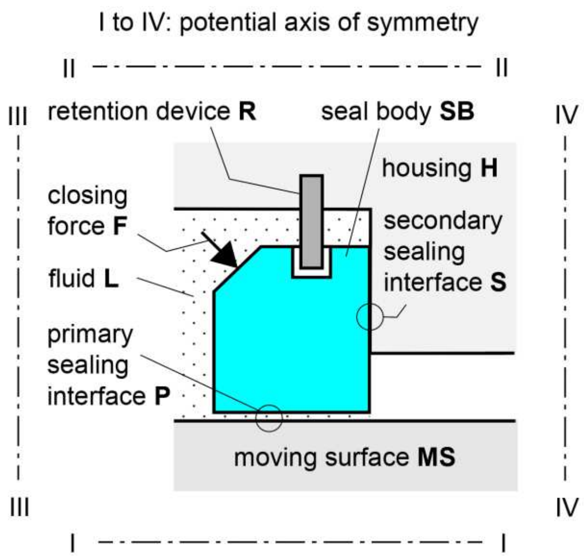

Figure 1: Schematic of a dynamic seal (adapted from [2]).

Maintaining the closing force between the counter surface and the sealing body is crucial for effective sealing. This is achieved by ensuring the total specific load (closing force minus the sealing interface area) exceeds the pressure of the sealed fluid. Figure 1 illustrates these closing forces as a combined closing force (F). Additional closing forces can be implemented, as demonstrated in Figure 2.

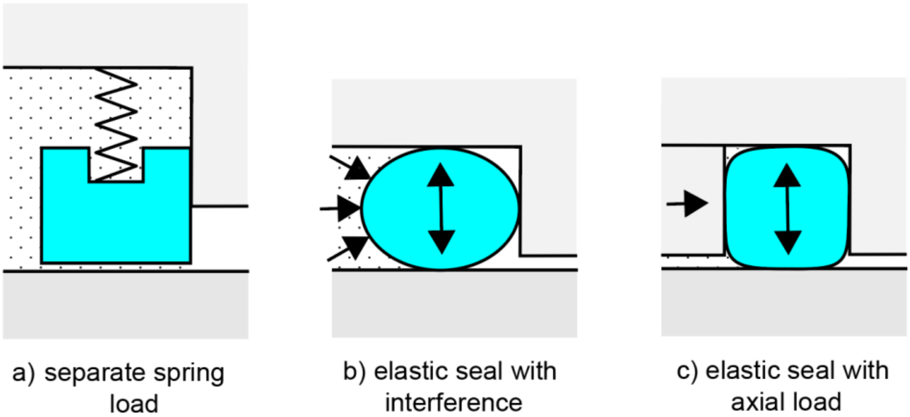

Figure 2: Examples of conventional preloading concepts (adapted from [2]).

Mechanical seals utilize compression springs (a) or bellows, which act as springs. Elastomeric seals can be preloaded through dimensional interference and elastic deformation of the seal itself (b). Soft packing rings are axially precompressed, creating a closing force at the sealing interface (c) [2].

Ideally, the closing force should compensate for wear and adapt to dynamic conditions. Some sealing solutions can adapt passively, due to different operational conditions linked to thermal expansion [2] and centripetal forces, which cause displacement and deformation [3]. Active adaptation is not yet available for conventional sealing technologies. This paper focuses on an active, adaptable contact force based on the concept of separate spring loading as shown in Figure 2a.

2.2 Shape-memory alloys (SMAs)

SMAs are a type of thermo-mechanical-transformation materials that are known for unique ability to switch between different atomic structures based on temperature. The most common compositions are copper-aluminum-nickel (CuAlNi) and nickel-titanium (NiTi), although they can also be synthesized using other elements like zinc, copper, gold and iron. While commercially available iron-based and copper-based SMAs (such as Fe-Mn-Si, Cu-Zn-Al, and Cu-Al-Ni) are more affordable, NiTi-based SMAs are preferred in most applications due to their stability and practicality [5] [6] [7].

The remarkable effects of SMAs arise from their ability to transition between the martensite and austinite phases. Martensite has a face-centered cubic structure with an atomic packing factor (APF) of 68 %, while austinite has a body-cantered cubic structure with an APF of 74 %, as shown in Figure 3. This phase transition causes a volume shift, with specific temperatures marking the start and finish of the transitions (M_s, M_f, A_s, A_f).

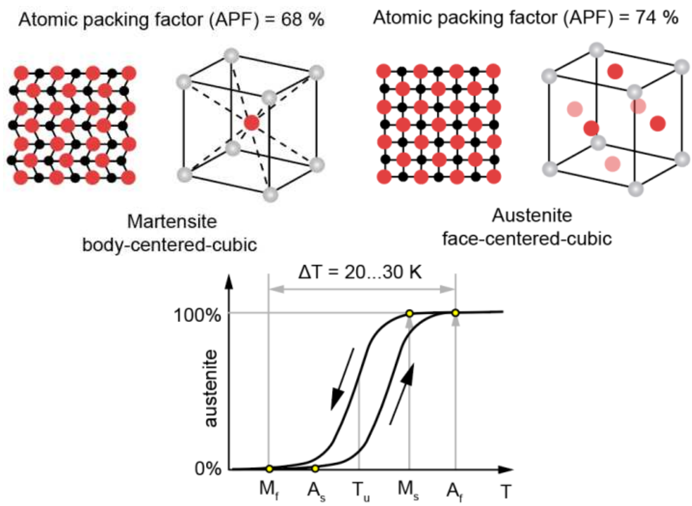

Figure 3: Transition from martensite to austenite (adapted from [4]).

In addition to temperature-induced effects, the martensite exhibits pseudo-plasticity, which is explained through a stress-strain-diagram and crystallography as shown in Figure 4. Initially, martensite exists in a twinned crystal structure (State A). Applying tension leads to elastic deformation, and at a specific tension (Point B), detwinning occurs. Heating the SMA above A_s and then cooling it reverses the deformation, re-twinning the martensite (pseudo-plasticity).

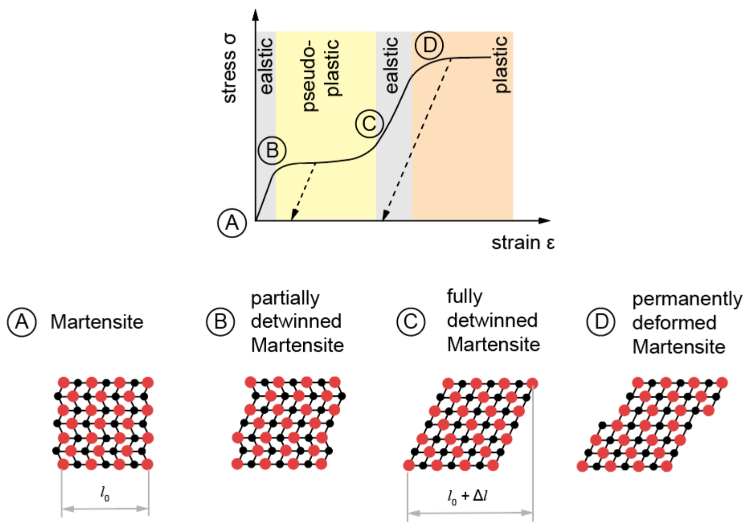

Figure 4: Pressure effects in the martensite structure (adapted from [4]).

Figure 5 shows how the combination of pseudo-plasticity and phase change can be used for the one-way effect. The material is pseudo-plastically deformed (A to C) and responds to a temperature shift with actuation (C to D). To repeat the actuation, the SMA must be cooled (D to A) and deformed again (A to C), with the material only memorizing the high-temperature austinite state. As to see in the diagram, a temperature increase from state A to D causes only a small change of deformation.

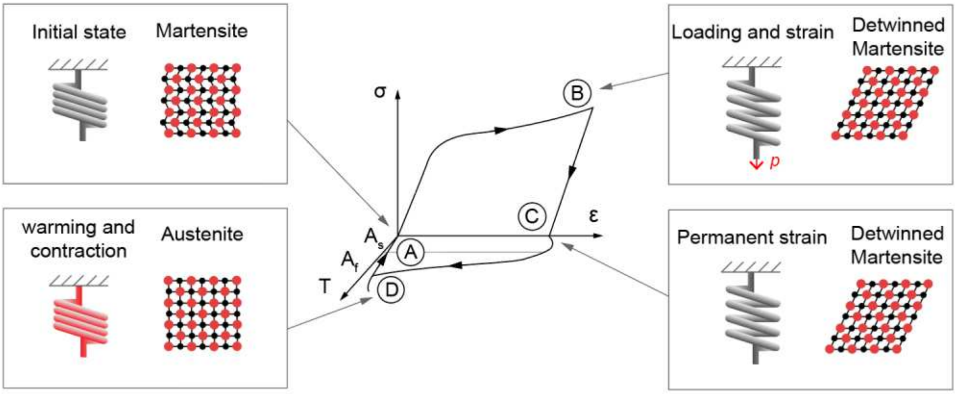

Figure 5: One-way effect (adapted from [4]).

For significant deformation between different temperatures, the two-way effect is necessary. This effect is achieved by training the SMA's microstructure through tension. The intrinsic material effect is shown in Figure 6, where the SMA cycles between detwinned martensite and austenite states. This effect can be enhanced under tension, known as the extrinsic two-way effect.

To increase pressure in the SMA, force can be applied, either by a constant force, or by an antagonist spring (Figure 7).

In this paper, the extrinsic two-way effect is used, in which the SMA is acting against a spring.

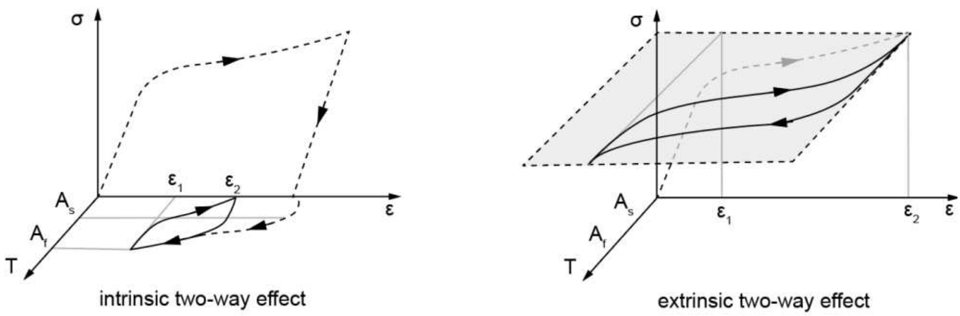

Figure 6: Two-way effect (adapted from [4]).

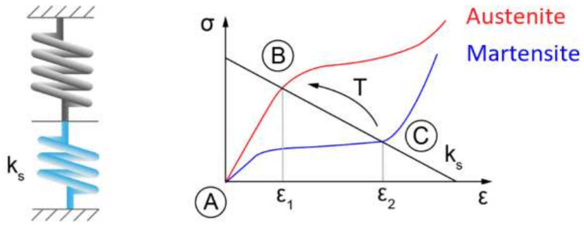

Figure 7: Two-way effect under variable force (adapted from [4]).

3 Test Set-up

The utilization of SMAs to adapt contact pressure was investigated through an experimental set-up. This process required several key steps:

- Selecting the appropriate SMA
- Developing an adaptable sealing concept
- Activating the smart energized seal
- Collecting data
- Establishing test procedures.

3.1 Selecting the appropriate SMA

The primary function of the SMA is to adjust the contact pressure of the chosen seal. It must be flexible and adaptable to various geometries. Key requirements for the SMA included shape-shifting at safe handling temperatures above ambient, availability in multiple sizes and a material that offers maximum design flexibility. A NiTiNol wire alloyed with NiTiCu was chosen, featuring an austinite finishing temperature of 60 °C (+/-5) and a thickness of 0.25mm and 0.5 mm.

3.2 Developing an adaptable sealing concept

The SMA serves as a smart energizer to adjust the radial load of a linear seal made from a bronze-filled PTFE compound. The seal's cross section is designed in a rectangular shape, as illustrated in Figure 8. The wire is positioned in a groove along the outer diameter of the rectangular ring. The wire ends are joined with a reef knot. Two different SMA wire thicknesses are chosen for placement in the groove:

- 0.25 mm
- 0.5 mm.

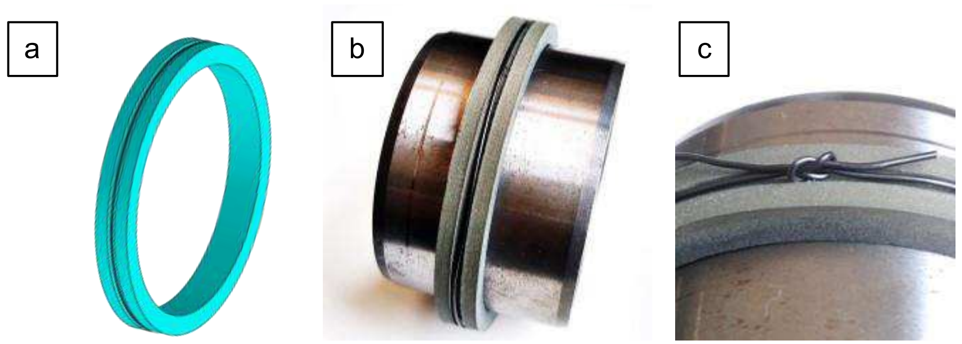

Figure 8: Design of the SMA actuated PTFE ring. a) CAD-PTFE ring with a groove, b) PTFE ring with SMA wire in the groove, c) reef knot of the SMA.

3.3 Activating the smart energized seal

The chosen SMA wire has a high nickel content, which gives it a relatively high magnetic permeability. This property makes it ideal for contactless, inductive heating, allowing for precise heating of the SMA wire compared to other heating methods.

The smart energized seal is primarily powered by a conventional laboratory power supply. The direct current from the power supply is converted into high frequency alternating current via an induction converter. This alternating current is then applied to a copper coil, which heats the SMA wire through induction.

3.4 Collecting data

The radial force of the smart energized seal is measured using a radial force measurement device in accordance with DIN 3761-9. Instead of employing a rod, the seal is mounted on two mandrels – one stationary and the other moveable, connected to a load cell. As the radial force of the seal increases, the gap between the mandrels decreases, causing deformation in the load cell. This load cell acts as a force-sensing resistor, which can be monitored using a voltage divider. The voltage signal is then amplified, recorded by a computer and displayed as a live graph. Figure 9 shows the test setup.

3.5 Establishing test procedures

For all experiments, the test setup shown in Figure 10 was used to examine the influence of the SMA wire on radial contact force. The success of these measurements hinged on two factors: observing significant thermal effects and ensuring the safety of personnel and equipment. To this end, only the necessary voltage was applied to the power supply for each measurement.

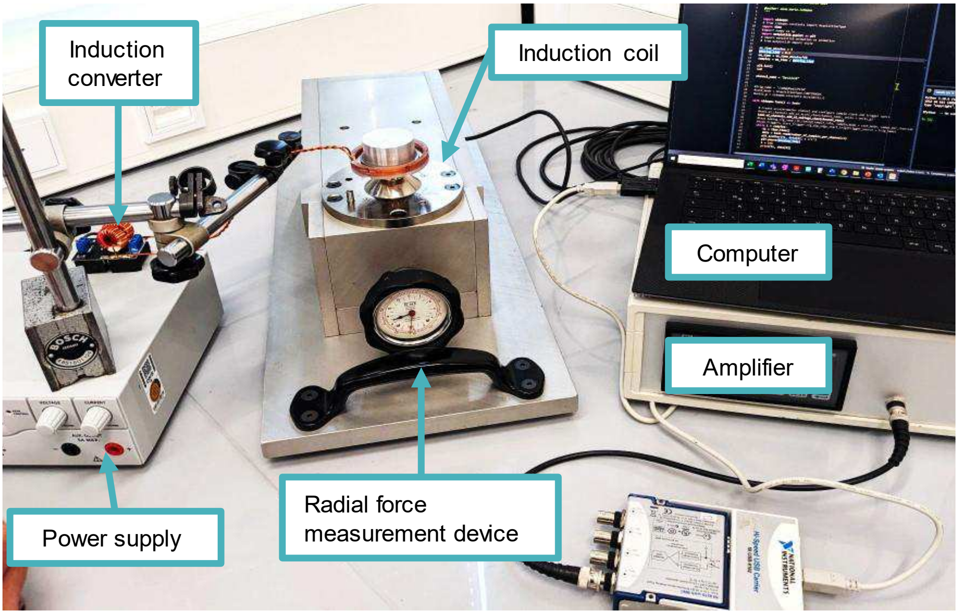

Figure 9: Test set-up for actuation and measuring the PTFE-SMA ring.

A human-in-the-loop approach was adopted, where an operator monitored the live graph, detected any unusual heat and adjusted the rotary knob of the power supply to balance safety requirements and data validity. The procedure involved switching on the power supply and observing the live graph until a notable change was detected. Two different wire sizes (0.25 mm and 0.5 mm) were tested and the tests were named accordingly:

- 0.25 actuated test
- 0.5 actuated test.

The second experiment aimed to determine whether the SMA wire could maintain a specific contact force. Here, the control loop was managed by a human operator, who monitored the live graph and adjusted the power supply accordingly. This experiment was conducted with the 0.5 mm-SMA wire and is referred to as the maintaining-force test. Results and Discussion

3.6 Results

Figure 10 shows the 0.25 actuated test and Figure 11 presents the results of the 0.5 actuated tests. Both tests begin with a measurement without activation. In the 0.25 actuated test, the radial force decreases with heating and increases again once the heating is stopped, allowing the set-up to cool passively by the environment. During the heating process from 20 to 53 s the graph shows a step-function.

Conversely, the result of the 0.5 actuated test shows an increase in contact pressure at the onset of heating and a decrease once the heating stops. The graph is smooth and reaches a similar level of radial force in the unactuated state after 7 s of passive cooling.

Figure 12 shows the maintaining-force test, which begins in an activated state. Similar to the 0.5 actuated test, stopping the heating after 17 s decreases the radial forces, which restarting it increases them. Stopping the heating again results in a rapid decrease in radial force to a level comparable to the last non-heated phase. It was possible to maintain a contact force of approximately 60 N for about 100 seconds, albeit with some noise.

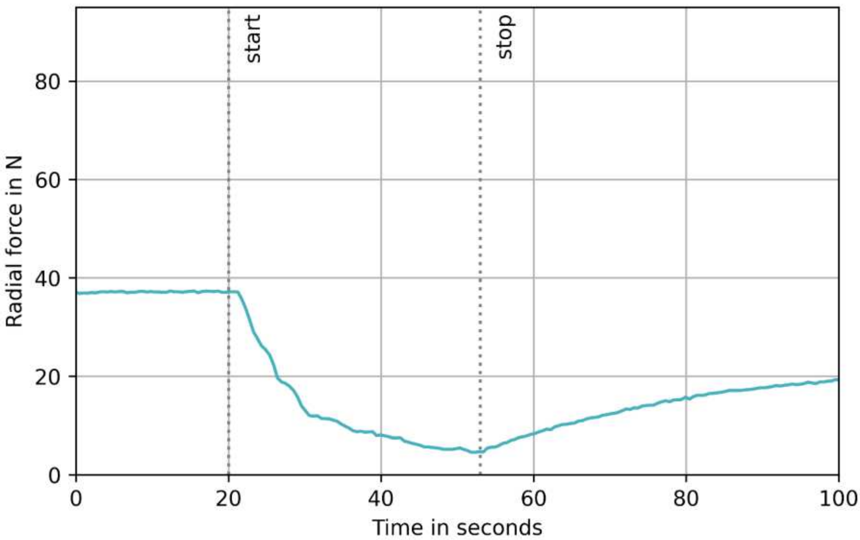

Figure 10: Radial force during heating a 0.25 mm SMA wire.

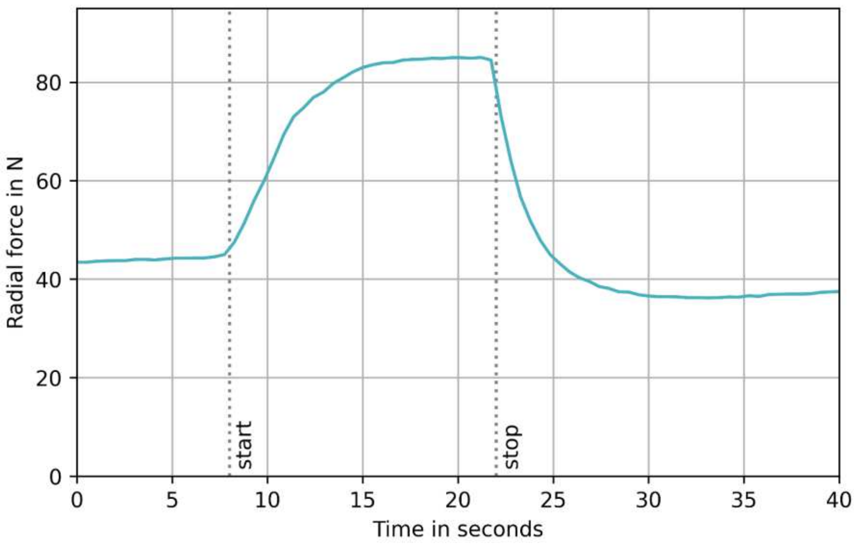

Figure 11: Radial force during heating a 0.5 mm SMA wire.

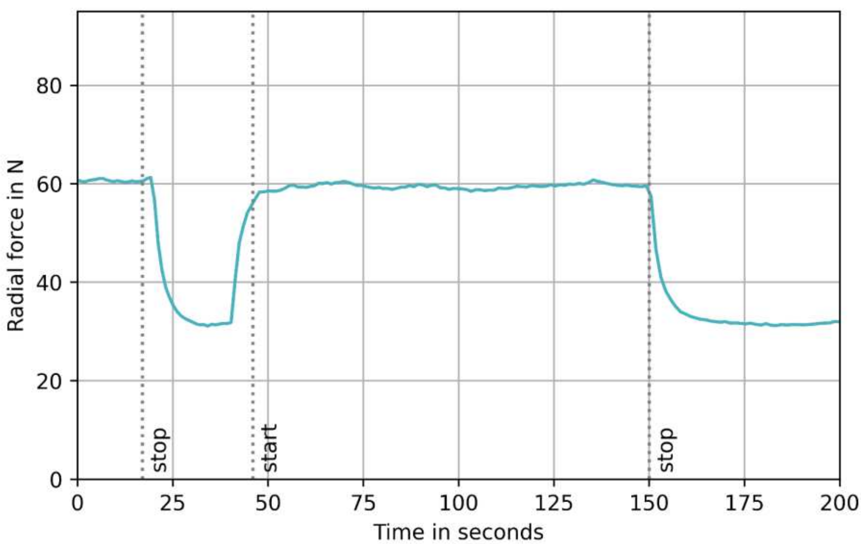

Figure 12: Test for maintaining contact pressure with 0.5 mm SMA wire.

3.7 Discussion

The test using a 0.5 mm SMA wire demonstrated an increase in radial force upon activation, while the 0.25 mm SMA wire showed a decrease. Maintaining a consistent contact pressure was possible in the activated state. Deactivating the 0.5 mm SMA wire led to a rapid return to the inactivated radial force level.

As illustrated in Figures 10-11, the thickness of the SMA wire significantly influences the qualitative effect on contact force. This is explained by the thermal behavior and the equilibrium of forces under thermal influence.

The displacement $u(r)$ of an annular ring disk, such as a PTFE ring, under a temperature shift ΔT and a relocatable outer boundary is given in Equation (1) and depends on the thermal expansion coefficients α_t.

Materials such as thermosets and steels typically have positive thermal expansion coefficient α_t, with steels generally expanding less then thermoplastics under heat. The thermal expansion of the mandrel or rod is therefore neglected in the analysis.

$$u(r) = \alpha_t \Delta T \; r \tag{1}$$

Notably, SMA's do not behave according to Equation (1) during their phase shift temperature; instead, they exhibit shrinkage as shown Chapter 2.1.

Assuming a linear time-invariant system and heating conditions within the SMA shift temperature range, the final radial force is a cumulation of forces, as shown in Figure 13. The expansion force of the PTFE opposes the shrinkage force of the SMA wire.

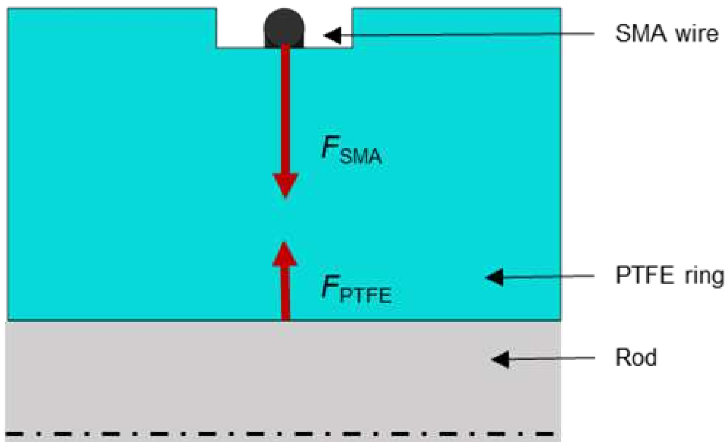

Figure 13: Direction of forces under heating.

The actuating volume of the SMA wire is strongly dependent on its diameter. Doubling the diameter results in a volume four times larger. Consequently, the force of the 0.5 mm SMA wire is therefore assumed to be four times stronger than that of the 0.25 mm SMA wire. This suggests that in the 0.25 actuated test, the SMA wire was not thick enough to counteract the thermal expansion of the PTFE ring; unlike the 0.5 mm wire, which increased the radial force upon activation.

Some artifacts of the human-in-the-loop control are evident in the graphs. During the 0.25 actuated test, the power was incrementally regulated. When the temperature exceeded the austinite finishing temperature of 60 °C, activation was halted. The 0.5 actuated test was regulated by gradually increasing the power output, resulting in smoother heating and cooling phases. During the force-maintaining test, the radial force was regulated to a specific level, this led to some noise generation.

There was a slight difference in radial force before and after stopping activation. Functions with high gradients are very sensitive to changes. Both SMAs and elastomers are known for their non-linear effects. Figure 7 simplistically shows how resulting deformations are set by the equilibrium of forces. Any slight change that might have occurred could alter the deformation states accordingly. Reasons for changes in the measured deformation might include the loosening of the reef knot, non-linear effects of SMA and PTFE, load cell drift, different cooling curves of the SMA wire and PTFE ring or insufficient recording time to reach a stationary unactuated cooling temperature.

4 Summary and Conclusion

For the first time, a test featuring a rectangular sealing ring and SMA was performed. Two different SMA wire thicknesses were evaluated. An induction coil setup was developed to facilitate the testing. Key findings revealed the importance of the sealing ring's thermal expansion and the necessity for the wire thickness to be suitable for the ring's cross-sectional dimensions. By manually controlling the input voltage, a consistent radial holding force was maintained. Performance parameters crucial to functionality, such as friction force and leakage – both dependent on radial force – can be utilized as signals to calculate adjustments for the SMA wire.

Sealing applications entail numerous requirements, the most critical being a compact installation space and ease of system assembly. For practical use, it is essential to thoroughly examine a system configuration that integrates feedback signals and meets these specific requirements.

5 Nomenclature

Variable	*Description*	*Unit*
A_f	austenite finishing temperature	°C
A_s	austenite starting temperature	°C
F	force	N
k	PTFE-spring stiffness	N/m
M_f	martensite finishing temperature	°C
M_s	martensite starting temperature	°C
$u(r)$	displacement under temperature shift	m
α_t	thermal expansion coefficient	$mm^{-1} K^{-1}$
ΔT	temperature shift	K
r	radius	m
ε	strain	%
σ	stress	Pa
NiTi	nickel-titanium	
NiTiCu	nickel-titanium-copper	
PTFE	polytetrafluoroethylene	
SMA	shape memory alloy	

6 References

[1] Winkler, H., Berger, U., Mieke C., Schenk, M.: *Flexibilisierung der Fabrik im Kontext von Industrie 4.0*, Logos Verlag Berlin GmbH, 2017.

[2] Müller, H., Nau, B.: *Fluid Sealing Technology: Principles and Applications*, Dekker, 1998.

[3] Schüle, C., Franz, M., Wehmann C., Amorim, S.: *Axial seal for high-rpm application and poor lubrication*. 21st International Sealing Conference 2022, Stuttgart, Germany, 2022.

[4] Sinapius, J. M.: *Adaptronik*, Springer Vieweg, Berlin, 2018.

[5] Cederström J., Van Humbeeck J.: *Relationship Between Shape Memory Material Properties and Applications*, In: *Journal de Physique IV,* 1995.

[6] Hodgson, D. E., Wu, M. H., B. R. J.: *Shape Memory Alloys, Properties and Selection: Nonferrous Alloys and Special-Purpose Materials,* 1990.

[7] Wilkes K. E., Liaw, P. K.: *The fatigue behavior of shape-memory alloys*, Springer, 2000.

[8] Kang, G., Yu, C., Kan, Q.: *Thermo-Mechanically Coupled Cyclic Deformation and Fatigue Failure of NiTi Shape Memory Alloys*, , Springer Singapore, 2023.

[9] Kang, G., Kan, Q., Qian L., Liu, Y.: *Ratcheting deformation of super-elastic and shape-memory NiTi alloys*, *Mechanics of Materials* 41.2: 139-153, 2009.

[10] Chaudhari, R., Vora, J. J., Parikh, D. M.: *A Review on Applications of Nitinol Shape Memory Alloy*, In: Recent Advances in Mechanical Infrastructure: Proceedings of ICRAM 2020 (2021): 123-132.

[11] Kang, G., Kan, Q., Yu, C., Liu, Y.: *Whole-life transformation ratchetting and fatigue of super-elastic NiTi alloy under uniaxial stress-controlled cyclic loading*, In: Materials Science and Engineering: A, 535, 228-234.

7 Authors

Trelleborg Sealing Solutions Germany

Schockenriedstraße 1, 70565 Stuttgart, Germany

Anne Marie Lehmann

ORCID 0009-0001-4299-6307, anne.marie.lehmann@trelleborg.com

Anja Dobrinsky

ORCID 0009-0002-0300-0535, anja.dobrinsky@trelleborg.com

Martin Franz

ORCID 0009-0008-0457-9116, martin.franz@trelleborg.com

https://doi.org/10.61319/D19MQHL2